The Astrophysical Journal, 581:501–508, 2002 December 10

STUDIES OF THE RELATIVISTIC BINARY PULSAR PSR B1534+12. I. TIMING ANALYSIS

I. H. Stairs
National Radio Astronomy Observatory, Green Bank, WV 24944; istairs@nrao.edu

S. E. Thorsett
Department of Astronomy and Astrophysics, University of California, Santa Cruz, CA 95064; thorsett@ucolick.org

J. H. Taylor
Joseph Henry Laboratories and Physics Department, Princeton University, Princeton, NJ 08544; joe@pulsar.princeton.edu

and

A. Wolszczan
Department of Astronomy and Astrophysics, Pennsylvania State University, University Park, PA 16802; alex@astro.psu.edu
Received 2002 July 2; accepted 2002 August 12

ABSTRACT

We have continued our long-term study of the double neutron star binary pulsar PSR B1534+12, using new instrumentation to make very high precision measurements at the Arecibo Observatory. We have significantly improved our solution for the astrometric, spin, and orbital parameters of the system as well as for the five "post-Keplerian" orbital parameters that can be used to test gravitation theory. The results are in good agreement with the predictions of general relativity. With the assumption that general relativity is the correct theory of gravity in the classical regime, our measurements allow us to determine the masses of the pulsar and its companion neutron star with high accuracy: $1.3332 \pm 0.0010\ M_\odot$ and $1.3452 \pm 0.0010\ M_\odot$, respectively. The small but significant mass difference is difficult to understand in most evolutionary models, as the pulsar is thought to have been born first from a more massive progenitor star and then undergone a period of mass accretion before the formation of the second neutron star. PSR B1534+12 has also become a valuable probe of the local interstellar medium. We have now measured the pulsar distance to be 1.02 ± 0.05 kpc, giving a mean electron density along this line of sight of 0.011 cm^{-3}. We continue to measure a gradient in the dispersion measure, though the rate of change is now slower than in the first years after the pulsar's discovery.

Subject headings: binaries: close — gravitation — pulsars: individual (PSR B1534+12) — stars: distances

1. INTRODUCTION

The discovery (Hulse & Taylor 1975) of the first pulsar in a binary system, PSR B1913+16, introduced the possibility of powerful new experimental tests of gravity in the strong field and radiative regimes. Over a quarter-century, measurements of this pulsar were shown to be in excellent agreement with the predictions of general relativity (Taylor & Weisberg 1989; Damour & Taylor 1991; Taylor 1994). A dozen years ago, the discovery (Wolszczan 1991) of PSR B1534+12—a bright, relatively nearby pulsar, also with a neutron star companion—promised the independent opportunity to confirm the tests of gravity done earlier with PSR B1913+16. Furthermore, B1534+12's favorable, nearly edge-on orbital geometry allowed new experimental tests that were complementary to those done with PSR B1913+16 (Taylor et al. 1992).

In earlier work (Stairs et al. 1998, hereafter Paper I), we analyzed data taken over a 6 yr period with the Arecibo 305 m telescope, the 43 m telescope at Green Bank, West Virginia, and the 76 m Lovell Telescope at Jodrell Bank Observatory, U.K. We found that those data were in agreement with the predictions of general relativity at the limit of the measurement uncertainties: about 1%. We showed that the orbital period was decreasing, as expected if the system is losing energy in the form of gravitational radiation. Because the observed orbital decay rate is contaminated by kinematic effects that depend on the unknown pulsar distance (Damour & Taylor 1991; Camilo, Thorsett, & Kulkarni 1994), the radiation predictions of general relativity cannot be tested with this pulsar to better than ~30% without an independent distance measurement. However, with the assumption that general relativity is the correct theory of gravity, we were able to invert the kinematic model to measure the pulsar distance to 20%.

Over the past 4 yr, we have continued our studies of PSR B1534+12, using the recently upgraded Arecibo telescope together with a new data acquisition system (Stairs et al. 2000a) that fully removes the dispersive effects of the interstellar medium from the signal. In addition to extending the length of the data set by more than half, these new data are of substantially higher quality than those available for Paper I. In this paper, we report on timing studies based on the complete 11.5 yr Arecibo data set. We present the improved tests of general relativity that are now possible, give a pulsar distance accurate to 5%, and report on dispersion measure variations. In subsequent papers, we will describe the analysis of secular variations in the pulsar radiation pattern that have been interpreted as evidence for geodetic precession of the pulsar, and we will discuss single-pulse studies.

2. OBSERVATIONS

In this paper, we discuss results of observations made with two different observing systems at the Arecibo telescope. Many of the details have already been discussed in Paper I and are only summarized here and in Table 1.

Observations were made with the 305 m Arecibo telescope both before its upgrade (1990–1994) and after its upgrade (1997–2002). For our purposes, the most important

TABLE 1
PARAMETERS OF THE FOUR OBSERVING SYSTEMS

Parameter	Mark III	Mark III	Mark IV	Mark IV
Frequency (MHz)	1400	430	1400	430
Bandwidth (MHz).....	40	8	5	5
Spectral channels	32	32	1	1
Dedispersing system...	Incoherent	Incoherent	Coherent	Coherent
Time resolution (μs) ...	97	329	38	38
Integration time (s).....	300	180	190	190
Dates	1990.8–94.1	1990.7–94.2	1998.6–2002.3	1997.9–2002.3
Number of TOAs	1185	2311	639	1635
Median $\sigma_{\rm TOA}$ (μs)	6.1	6.0	6.7	4.2

postupgrade change was a significant reduction in the system temperature at 1400 MHz, leading to an improvement in the signal-to-noise ratio achieved for a given integration time and observing bandwidth. During the period that the Arecibo telescope was unavailable, observations were made with the National Radio Astronomy Observatory (NRAO) 43 m telescope at Green Bank and with the 76 m Lovell telescope at Jodrell Bank Observatory, UK. The latter two data sets were used in Paper I, but with the abundance of high-quality postupgrade Arecibo data, they contribute nothing to the present solution and are therefore disregarded in this work.

Two observing systems were used. The Princeton Mark III system (Stinebring et al. 1992) is an "incoherent" system in which the incoming signal is decomposed into spectral channels with a filter bank. The effective time resolution is dominated by dispersion smearing of the signal during its propagation through the ionized interstellar medium, with some additional instrumental smoothing after detection of the signal. The signals in each frequency channel were folded at the instantaneous topocentric pulsar period for 3–5 minutes, then the channels were shifted to account for interstellar dispersion and summed to produce a single total-intensity (summed polarization) pulse profile for each integration.

For the new postupgrade data that we introduce here, we observed with a "coherent" system: the Princeton Mark IV instrument (Stairs et al. 2000a). For each sense of circular polarization, a 5 MHz bandpass was mixed to baseband using local oscillators in phase quadrature. The four resulting signals were low-pass filtered at 2.35 MHz, sampled at 5 MHz with 4 bit quantization, and written to a large disk array. Some of the 1400 MHz observations were taken with 10 MHz of bandwidth and 2 bit quantization. In the off-line processing, the undetected signal voltages were dedispersed using the phase-coherent technique described by Hankins & Rickett (1975). After amplitude calibrations were applied, self- and cross-products of the right- and left-handed complex voltages yielded the Stokes parameters of the incoming signal. These products were folded at the topocentric pulsar period using 1024 phase bins, and pulse TOAs were determined from the resulting total-intensity profiles. A summary of the more important parameters and statistics of all combinations of observing systems and frequencies is presented in Table 1. Many of the postupgrade data come from observations on 1 or 2 days at quasi-regular intervals; in addition, we conducted 12 day intensive "campaign-style" observations in each of the summers of 1998, 1999, 2000, and 2001, with full orbital coverage at each epoch. This mixture of data permits a high-quality timing solution and allows us to monitor, at each campaign epoch, the pulse shape changes due to geodetic precession, which we will discuss in a subsequent paper.

As in Paper I, we used the same TOA-fitting procedure for all data sets. Each observed profile was fitted to a standard template, using a least-squares method in the Fourier transform domain (Taylor 1992) to measure its time offset. The offset was added to the time of the first sample of a period near the middle of the integration, thereby yielding an effective pulse arrival time. A different standard template was used for each observing system and frequency: they were made by averaging the available profiles over several hours or more. Uncertainties in the TOAs were estimated from the least-squares procedure, and a minimum error, dependent on the observing system and frequency, was required for each TOA. In addition, a cut was established such that nearly all Mark IV TOAs with least-squares uncertainties greater than 10 μs (roughly 20% of the data) were discarded: tests show that they do not significantly affect the best-fit solution or the parameter uncertainties, and discarding these data points allows us to better assess the data quality (§ 3.3). The observatory's local time standard was corrected retroactively to the UTC timescale using data from the Global Positioning System (GPS) satellites.

3. DATA ANALYSIS

3.1. *The Timing Model*

A pulse received on Earth at topocentric time t is emitted at a time in the comoving pulsar frame given by

$$T = t - t_0 + \Delta_C - D/f^2 + \Delta_{R\odot} + \Delta_{E\odot} - \Delta_{S\odot} - \Delta_R - \Delta_E - \Delta_S \ . \quad (1)$$

Here t_0 is a reference epoch and Δ_C is the offset between the observatory master clock and the reference standard of terrestrial time. The dispersive delay is D/f^2, where $D = {\rm DM}/2.41 \times 10^{-4}$, with the dispersion measure DM in cm^{-3} pc, the radio frequency f in MHz, and the delay in seconds. The $\Delta_{R\odot}$, $\Delta_{E\odot}$, and $\Delta_{S\odot}$ terms are propagation delays and relativistic time adjustments for effects within the solar system, and Δ_R, Δ_E and Δ_S are similar terms accounting for phenomena within the pulsar's orbit.

In Paper I, we set out the equations that define the three orbital terms Δ_R, Δ_E, and Δ_S in terms of 10 parameters. Five are the standard Keplerian parameters: the period P_b, projected semimajor axis $x \equiv a_1 \sin i/c$, eccentricity e, longitude

of periastron ω, and time of periastron T_0. The other five are post-Keplerian (PK) parameters: the rate of advance of the periastron $\dot{\omega}$, orbital period derivative $\dot{P}_b$, time dilation and gravitational redshift γ, and range r and shape s of the Shapiro time delay. These quantities, in conjunction with the time-variable dispersion measure, a simple time polynomial to model the spin of the pulsar, and astrometric parameters to model the propagation of the signal across the solar system constitute the free parameters to be fitted in the theory-independent timing model.

Within the framework of a particular theory of gravity, the five PK parameters can be written as functions of the pulsar and companion star masses, m_1 and m_2, and the well determined Keplerian parameters. In general relativity, the equations are as follows (see Damour & Deruelle 1986; Taylor & Weisberg 1989; Damour & Taylor 1992):

$$\dot{\omega} = 3\left(\frac{P_b}{2\pi}\right)^{-5/3} (T_\odot M)^{2/3}(1-e^2)^{-1}, \quad (2)$$

$$\gamma = e\left(\frac{P_b}{2\pi}\right)^{1/3} T_\odot^{2/3}\ M^{-4/3}\ m_2\ (m_1+2m_2), \quad (3)$$

$$\dot{P}_b = -\frac{192\pi}{5}\left(\frac{P_b}{2\pi}\right)^{-5/3}\left(1+\frac{73}{24}e^2+\frac{37}{96}e^4\right) \times (1-e^2)^{-7/2}\ T_\odot^{5/3}\ m_1\ m_2\ M^{-1/3}, \quad (4)$$

$$r = T_\odot\ m_2, \quad (5)$$

$$s = x\left(\frac{P_b}{2\pi}\right)^{-2/3} T_\odot^{-1/3}\ M^{2/3}\ m_2^{-1}. \quad (6)$$

Here the masses m_1, m_2, and $M \equiv m_1 + m_2$ are expressed in solar units, $T_\odot \equiv GM_\odot/c^3 = 4.925490947\ \mu$s, G the Newtonian constant of gravity, and c the speed of light.

3.2. *Arrival Time Analysis*

We used the standard TEMPO analysis software (Taylor & Weisberg 1989)[1] together with the JPL DE200 solar system ephemeris (Standish 1990) to perform a least-squares fit of the measured pulse arrival times to the timing model. Results for the astrometric, spin, and dispersion parameters of PSR B1534+12 are presented in Table 2. The DM was fitted in two blocks, pre- and postupgrade, with different base values and time derivatives in each block. Because of systematic errors (see § 3.3 below), the Mark III 430 MHz data were only used to fit the preupgrade DM and DM derivative and were not incorporated into the rest of the timing solution. This meant that an iterative approach was required to find the best-fit DMs: first the spin and orbital solution was held constant, while the DM parameters were fitted using the whole data set, then the Mark III 430 MHz data were dropped as the best overall timing solution was obtained from the other data, holding the preupgrade DM parameters fixed. This new timing solution was then used to refine both sets of DM parameters until no significant changes resulted. The DM and DM derivative uncertainties reported in Table 2 are the errors derived while holding the rest of the timing solution fixed. Fitting for postupgrade DM and DM-derivative simultaneously with the rest of the timing solution yielded similar values, but somewhat larger uncertainties due to covariances with other parameters. Figure 1 shows the time variation of the best-fit DM, with the DM and first derivative from Paper I shown for comparison; the preupgrade values are consistent within the uncertainties.

[1] See also http://pulsar.princeton.edu/tempo.

TABLE 2

Astrometric, Spin, and Dispersion Parameters for PSR B1534+12

Parameter	Value
Right ascension, α (J2000)	$15^h37^m09^s.960312(10)$
Declination, δ (J2000)	$11^\circ55'55''.5543(2)$
Proper motion in R.A., μ_α (mas yr^{-1})	1.32(3)
Proper motion in decl., μ_δ (mas yr^{-1})	−25.12(5)
Parallax, π (mas)	<1.5
Pulse period, P (ms)	37.9044407982695(4)
Period derivative, $\dot{P}$ (10^{-18})	2.422622(3)
Epoch (MJD)	50261.0
Dispersion measure, DM, 1 (cm^{-3} pc)	11.61944(2)
DM derivative 1 (cm^{-3} pc yr^{-1})	−0.000316(10)
DM Epoch 1 (MJD)	48778.0
DM 2 (cm^{-3} pc)	11.61634(3)
DM derivative 2 (cm^{-3} pc yr^{-1})	−0.000073(7)
DM Epoch 2 (MJD)	51585.0
Galactic longitude l (deg)	19.8[a]
Galactic latitude b (deg)	48.3[a]
Composite proper motion, μ (mas yr^{-1})	25.15(5)[a]
Galactic position angle of μ (deg)	239.16(8)[a]

Note.—Values in parentheses are uncertainties in the last digits quoted.

[a] Derived quantities.

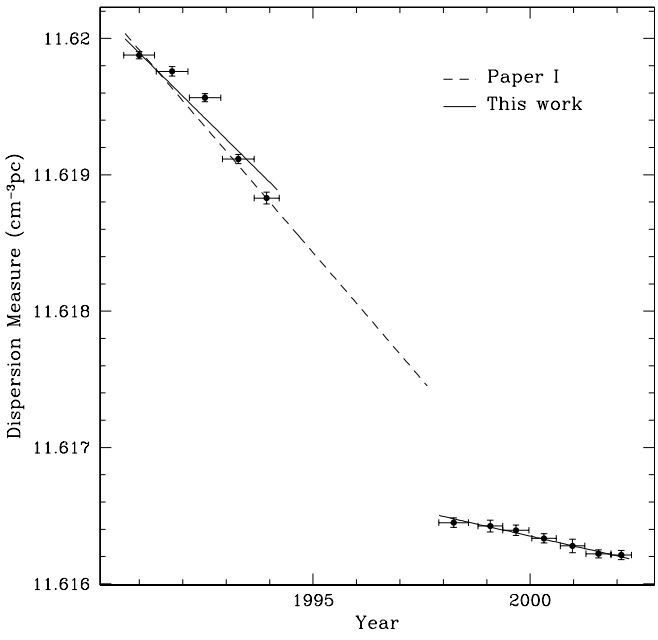

Fig. 1.—Dispersion measure (DM) used in the fits presented in Tables 2 and 3. Different values and derivatives are needed for the pre- and postupgrade data sets. The DM and its variation obtained in Paper I are shown for comparison: they match our current results within the uncertainties. Points with error bars illustrate the quality of DM fits over short intervals. *Horizontal error bars*: Domain of each fit. *Vertical error bars*: Uncertainties derived in each time bin.

TABLE 3
ORBITAL PARAMETERS OF PSR B1534+12 IN THE DD AND DDGR MODELS

Parameter	DD Model	DDGR Model
Orbital period, P_b (days)	0.420737299122(10)	0.420737299123(10)
Projected semimajor axis, x (s)	3.729464(2)	3.7294641(4)
Eccentricity, e	0.2736775(3)	0.27367740(14)
Longitude of periastron, ω (deg)	274.57679(5)	274.57680(4)
Epoch of periastron, T_0 (MJD)	50260.92493075(4)	50260.92493075(4)
Advance of periastron, $\dot{\omega}$ (deg yr^{-1})	1.755789(9)	1.7557896[a]
Gravitational redshift, γ (ms)	2.070(2)	2.069[a]
Orbital period derivative, $(\dot{P}_b)^{\rm obs}$ (10^{-12})	−0.137(3)	−0.1924[a]
Shape of Shapiro delay, s	0.975(7)	0.9751[a]
Range of Shapiro delay, r (μs)	6.7(1.0)	6.626[a]
Derivative of x, $\lvert\dot{x}\rvert$ (10^{-12})	<0.68	<0.015
Derivative of e, $\lvert\dot{e}\rvert$ (10^{-15} s^{-1})	<3	<3
Total mass, $M = m_1 + m_2$ ($M_\odot$)	...	2.678428(18)
Companion mass, m_2 ($M_\odot$)	...	1.3452(10)
Excess $\dot{P}_b$ (10^{-12})	...	0.055(3)

Note.—Figures in parentheses are uncertainties in the last digits quoted.
[a] Derived parameters, assuming general relativity.

We note that the offset in DM base values between the pre- and postupgrade fits is due mostly to the use of different standard profiles with necessarily different frequency alignments; thus, this offset should not be interpreted as physically meaningful. The change in DM *derivative*, however, is real and is discussed in § 4.2 below. An arbitrary time offset was also allowed between the pre- and postupgrade data sets to accommodate the different standard profiles and changes in the instrumental signal path length.

Two models of the pulsar orbit were used to fit the data. The theory-independent DD model (Damour & Deruelle 1986) treats all five PK parameters defined in § 3.1 as free parameters in the fit. The alternate DDGR model (Taylor 1987; Taylor & Weisberg 1989) assumes that general relativity is correct and uses equations (2)–(6) to tie the PK parameters to $M \equiv m_1 + m_2$ and m_2; consequently, it requires only two post-Keplerian free parameters.

Table 3 presents our best-fit orbital parameters. Uncertainties given in the table are approximately twice the formal 1 σ errors from the fit. We believe them to be conservative estimates of the true 68% confidence uncertainties, including both random and systematic effects. For each model, we list the Keplerian parameters and the relevant post-Keplerian parameters. We also include in italic numbers the computed PK parameters derived from the measured masses in the DDGR fit—these computed parameters are in excellent agreement with the DD fit values. As in Paper I, the DDGR solution includes the "excess $\dot{P}_b$" parameter, which accounts for an otherwise unmodeled acceleration resulting from galactic kinematics. We note that the measured orbital period derivative, $-0.137 \pm 0.003 \times 10^{-12}$, is very close to the sum of the DDGR model's intrinsic value, -0.1924×10^{-12}, and the fitted excess, $+0.055 \pm 0.003 \times 10^{-12}$.

Figure 2 shows the postfit residuals for the preupgrade 1400 MHz data and the postupgrade 1400 and 430 MHz data plotted as functions of date. Interstellar scintillation causes the TOA uncertainties to vary somewhat, but in the interest of clarity, we have not drawn error bars on these residual plots. Figure 3 illustrates the averaged postfit residuals for the same data sets, plotted as functions of orbital phase.

3.3. *Comparison of Coherent and Incoherent Observing Systems*

As discussed in Paper I, solutions for the fitted parameters of PSR B1534+12, as determined from the preupgrade 430 MHz data, are biased by small systematic errors in the TOAs, likely caused by imperfect postdetection dispersion removal combined with variable interstellar scintillation patterns. These measurements are unreliable at the several

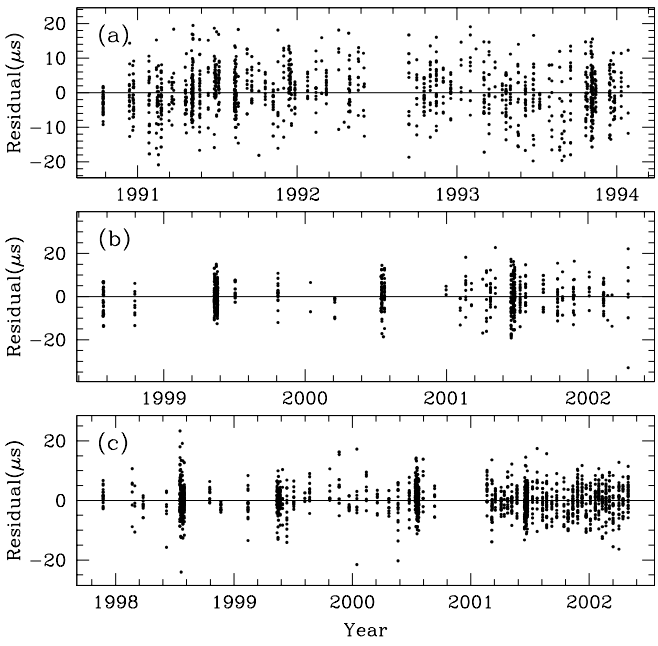

FIG. 2.—Postfit residuals vs. date for (*a*) preupgrade (Mark III) 1400 MHz data, (*b*) postupgrade (Mark IV) 1400 MHz data, and (*c*) postupgrade (Mark IV) 430 MHz data.

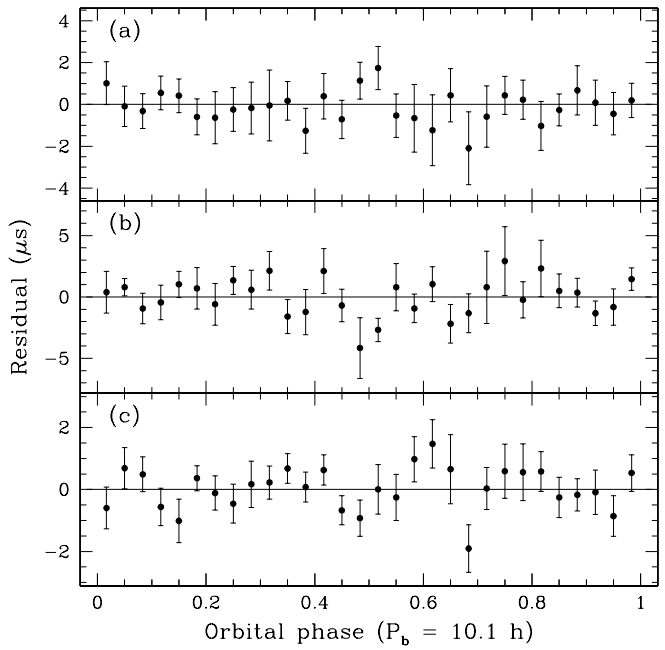

FIG. 3.—Average postfit residuals as a function of orbital phase for (*a*) preupgrade (Mark III) 1400 MHz data, (b) postupgrade (Mark IV) 1400 MHz data, and (*c*) postupgrade (Mark IV) 430 MHz data.

microsecond level required for high-precision timing of this pulsar.

One of our major goals in building the Princeton Mark IV instrument (Stairs et al. 2000a) was to improve the timing accuracy at low frequencies for fast systems such as PSR B1534+12 by minimizing any dispersion-related systematic errors in TOAs. We have determined that the new instrument does indeed appear to have circumvented the residual dispersion problems that plague the Mark III data at low frequencies. In Figure 4, we follow Taylor & Weisberg (1989) and Paper I in examining the statistical properties of the postfit residuals (relative to the solution of Tables 2 and 3) to see if they "integrate down" as $n^{-1/2}$ when n consecutive values are averaged. The preupgrade 1400 MHz data and both postupgrade data sets are fairly consistent with the expected slope, while the preupgrade 430 MHz data deviate significantly. This confirms that we have been justified in leaving the preupgrade 430 MHz data out of our preferred timing solution, that these Mark III 430 MHz data indeed contain systematic errors related to the incoherent dispersion removal, and that the new Mark IV instrument greatly reduces these systematics, as we had hoped. The minimum TOA uncertainty requirement mentioned above was introduced to compensate for the small remaining deviations from the $n^{-1/2}$ law visible in the three good data sets.

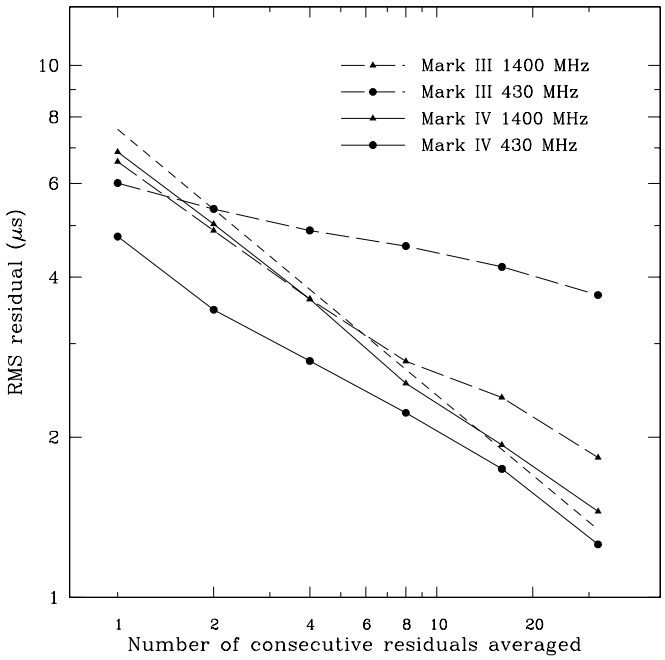

FIG. 4.—Root mean square (rms) residual vs. number of consecutive residuals averaged for the four data sets: preupgrade (Mark III) and postupgrade (Mark IV) data at each of 1400 and 430 MHz. *Short-dashed line*: Expected slope of $-1/2$ for uncorrelated residuals. All data sets except the preupgrade 430 MHz data are in reasonable agreement with this prediction.

4. DISCUSSION

4.1. *Observed Change in Orbital Period: Distance to PSR B1534+12*

The observed $\dot{P}_b$ is measured in the reference frame of the solar system barycenter and must be corrected to the center-of-mass frame of the binary pulsar system before it can be compared to the value predicted by GR. The largest correction is kinematic, involving the relative acceleration of the two reference frames. It can be broken down into the vertical acceleration in the Galactic potential, acceleration in the plane of the Galaxy, and an apparent centripetal acceleration due to the transverse velocity of the pulsar binary (Damour & Taylor 1991):

$$\left(\frac{\dot{P}_b}{P_b}\right)^{\rm gal} = -\frac{a_z \sin b}{c} - \frac{v_0^2}{cR_0}\left(\cos l + \frac{\beta}{\sin^2 l + \beta^2}\right) + \mu^2 \frac{d}{c} \ . \tag{7}$$

Here a_z is the vertical component of galactic acceleration, l and b the pulsar's galactic coordinates, R_0 and v_0 the Sun's galactocentric distance and galactic circular velocity, μ and d the pulsar's proper motion and distance, and $\beta = d/R_0 - \cos l$. As we do not have a precise distance to the pulsar through either a timing or an interferometric parallax measurement, the best independent distance estimate still comes from the Taylor & Cordes (1993) model of the free electron content of the Galaxy: this model puts the pulsar at a distance of 0.7 ± 0.2 kpc. At this distance, the Kuijken & Gilmore (1989) model of the Galactic potential yields an estimate of $a_z/c = (1.60 \pm 0.13) \times 10^{-19}$ s^{-1}. We assume $v_0 = 222 \pm 20$ km s^{-1} and $R_0 = 7.7 \pm 0.7$ kpc, as in Damour & Taylor (1991). Then, summing the terms in equation (7) and multiplying by P_b, we find the total kinematic bias to be

$$\left(\dot{P}_b\right)^{\rm gal} = (0.037 \pm 0.011) \times 10^{-12} \ . \tag{8}$$

The uncertainty in this correction is dominated by the uncertainty in distance, which is only roughly estimated by the Taylor and Cordes model. The slight decrease in the uncertainty from that given in Paper I results from an

increase by a factor of 10 in the precision of the proper motion measurement.

Our measurement of the intrinsic rate of orbital period decay is therefore

$$\left(\dot{P}_b\right)^{\rm obs} - \left(\dot{P}_b\right)^{\rm gal} = (-0.174 \pm 0.011) \times 10^{-12} \ . \quad (9)$$

The uncertainty is completely dominated by the uncertainty on the kinematic correction, which is nearly a factor of 4 larger than the measurement uncertainty on $\dot{P}_b^{\rm obs}$. In GR, the orbital-period decay due to gravitational radiation damping, $(\dot{P}_b)^{\rm GR}$, can be predicted from the masses m_1 and m_2 (eq. [4]), which in turn can be deduced from the high-precision measurements of $\dot{\omega}$ and γ. As listed in Table 3, the expected value is

$$\left(\dot{P}_b\right)^{\rm GR} = -0.192 \times 10^{-12} \ . \quad (10)$$

As in Paper I, our measured value differs from this prediction, now by some 1.7 standard deviations, and again, assuming that GR is the correct theory of gravity, we can derive the true distance to the pulsar from the "excess $\dot{P}_b$" parameter and equation (7) above (Bell & Bailes 1996). Our improved distance is $d = 1.02 \pm 0.05$ kpc (68% confidence limit). The uncertainty is still dominated by the measurement uncertainty of $(\dot{P}_b)^{\rm obs}$ rather than uncertainties in the galactic rotation parameters or the acceleration a_z, though the Galactic model uncertainties will ultimately limit the distance measurement to a few percent accuracy. The timing parallax for this system is still not significantly measured but is constrained to be less than 1.5 mas, in good agreement with the GR-derived result.

Our new distance result is consistent with the 1.1 ± 0.2 kpc determined in Paper I, but we have improved the uncertainty by a factor of 4. Our previous distance led to a downward revision of the estimated double neutron star inspiral rate visible to gravitational-wave observatories such as Laser Interferometer Gravitational-Wave Observatory. The new measurement leads to a small (15%) increase in the number density of similar systems in the local universe, with the uncertainty now dominated by the uncertain scale height of such binaries (Kalogera et al. 2001).

4.2. *Dispersion Measurements and the Local Interstellar Medium*

As noted in § 3.2, we find a significantly different DM and DM derivative in the postupgrade era than before the upgrade (Fig. 1). We argue that while the change in reference DM value is largely due to the use of new standard profiles with a slightly different frequency alignment, the difference in the rate of change (more than a factor of 4 slower since the upgrade) is physical. It is true that the profile at both frequencies is undergoing a secular evolution due to geodetic precession of the pulsar's spin axis (Arzoumanian 1995; I. H. Stairs et al., in preparation) and, thus, one might suspect a contribution to the DM derivative from different temporal evolution at the two observing frequencies. We explore this possibility by calculating the DM difference between our 1999 May and 2001 June observing campaigns, for the best-fit postupgrade DM derivative versus the best-fit *preupgrade* DM derivative, finding that if the preupgrade DM trend had continued, the 2001 June DM would have been smaller by about 0.0005 cm^{-3} pc. This large a difference would imply a difference in offset between the 430 and 1400 MHz profiles of 10 μs, or 0.27 bins in a 1024 bin profile. By comparing the actual cumulative profiles at these epochs using the same cross-correlation algorithm used to calculate TOAs, we estimate that the 430–1400 MHz offset has shifted by no more than about 0.05 bins. As the TOAs are determined by the strong main peak of the pulse, and the most noticeable evolution is taking place in the low-level emission near the base of the pulse (Stairs et al. 2000b), this is perhaps not surprising. We therefore conclude that the observed changes in DM slope do represent changes in the structure of the interstellar medium between the Earth and the pulsar.

With our current data set, it is not possible to construct a satisfactory structure function with which to characterize the length scales of turbulence in the interstellar medium (Phillips & Wolszczan 1991). Because of strong refractive scintillation at 1400 MHz, the high-frequency data set remains quite sparse (Fig. 2). Even though we may use a wider bandwidth instrument such as the recently commissioned 100 MHz Wideband Arecibo Pulsar Processor (WAPP) spectrometer for future 1400 MHz observations, the broadband nature of the refractive interstellar scintillation may make it difficult to accurately sample the dispersion measure variations with resolution finer than roughly 6 months.

4.3. *The Neutron Star Masses: Testing Evolutionary Theory*

The best mass estimates for the two neutron stars in the PSR B1534+12 system come from the DDGR timing model. The measured values are $m_1 = 1.3332 \pm 0.0010\ M_\odot$ and $m_2 = 1.3452 \pm 0.0010\ M_\odot$. The masses derived from the DD model and equations (5) and (6) are in good agreement with these values, though the measurement uncertainties are much larger (Fig. 5).

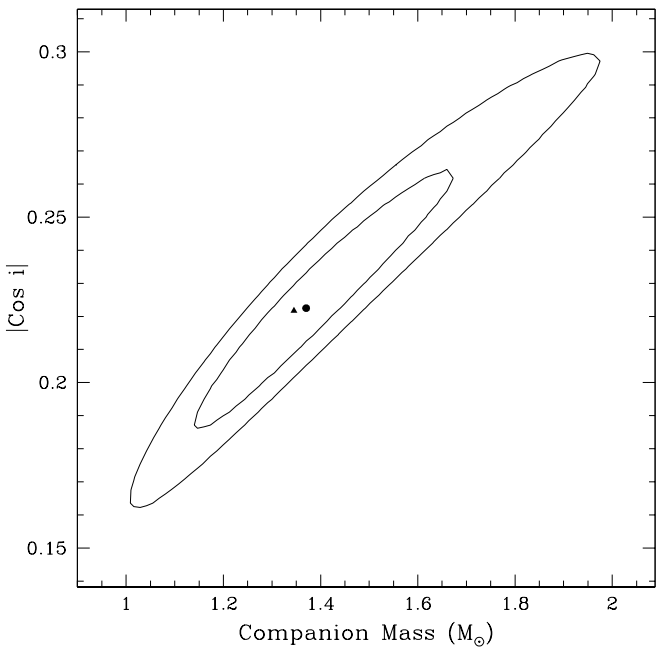

FIG. 5.—Shapiro delay parameters. *Contours*: Confidence levels ($\Delta\chi^2 = 1.0, 4.0$) for the companion mass and the cosine of the orbital inclination. *Round dot*: Best-fit DD solution in Table 3. *Triangle*: Optimal DDGR solution, which is well within the 68% contour of the DD solution.

Although the masses of the two neutron stars are very similar, it is now clear that the pulsar is significantly less massive than its companion. This is contrary to initial expectations from binary evolution. The pulsar is rapidly spinning and has the low magnetic field characteristic of a "recycled pulsar" that has been spun-up by mass transfer from a companion star. Assuming a monotonic relation between progenitor mass and neutron star mass, we therefore might predict that the pulsar would be more massive at birth and that the mass difference would only increase during the later evolution of the system.

This perhaps naive prediction has already been challenged by the binary pulsar system PSR B2303+46. Recently, the companion in this close, eccentric binary was shown to be a white dwarf rather than a second neutron star (van Kerkwijk & Kulkarni 1999). The eccentric orbit implies that the white dwarf formed first, from the star that was originally more massive. Presumably, mass transfer to the initially less massive star pushed it above the minimum mass needed to form a supernova and a neutron star.

A similar process may have been important in the formation of the PSR B1534+12 system. Although the pulsar was formed from the initially more massive star, mass transfer to its companion star probably resulted in a mass inversion before either neutron star was formed.

To move beyond the simplest (or most naive) predictions about the relative masses of the pulsar and companion in the B1534+12 system requires significant improvements in our theoretical understanding of several areas of stellar and binary evolution. First, we must understand the relationship between progenitor and neutron star masses, which may not be purely monotonic. Then we must understand how the mass lost by the pulsar's progenitor or gained by the companion's progenitor affected the evolution of the stellar cores and the amount of fallback during the supernova events. Finally, we must understand in some detail the mass transfer that spun up the pulsar. Although these are all challenging problems, there is some hope for future guidance from the growing number of precisely measured neutron star masses.

4.4. *Test of Relativity*

PSR B1534+12 permits the second test of general relativity based on the $\dot{\omega}$, γ, and $\dot{P}_b$ parameters of a binary pulsar system and adds significant measurements of the Shapiro delay parameters r and s. The left-hand sides of equations (2)–(6) represent quantities measured in a theory-independent fashion and listed in the DD column of Table 3. If GR is consistent with these measurements and there are no significant unmodeled effects, the five curves corresponding to equations (2)–(6) should intersect at a single point in the m_1-m_2 plane. These curves are presented in Figure 6, in which a pair of lines delimit the 68% confidence limit for each PK parameter (a single line is drawn for $\dot{\omega}$, whose uncertainty is too small to show). It is clear that the $\dot{\omega}$, γ, r, and s curves intersect, though r is still poorly measured. The curve obtained from the observed DD value of $\dot{P}_b$ can be made to intersect the others, as discussed above, by setting the pulsar distance to 1.02 ± 0.05 kpc rather than the 0.7 ± 0.2 kpc estimated from the dispersion measure. A filled circle at $m_1 = 1.3332\ M_\odot, m_2 = 1.3452\ M_\odot$ marks the DDGR solution of Table 3, and its location on the $\dot{\omega}$ line agrees to within 0.05% with the measured DD values of γ and s. This provides a highly precise test of the validity of general relativity using only nonradiative timing parameters, an important complement to the mixed $\dot{\omega}$–γ–$\dot{P}_b$ test provided by PSR B1913+16.

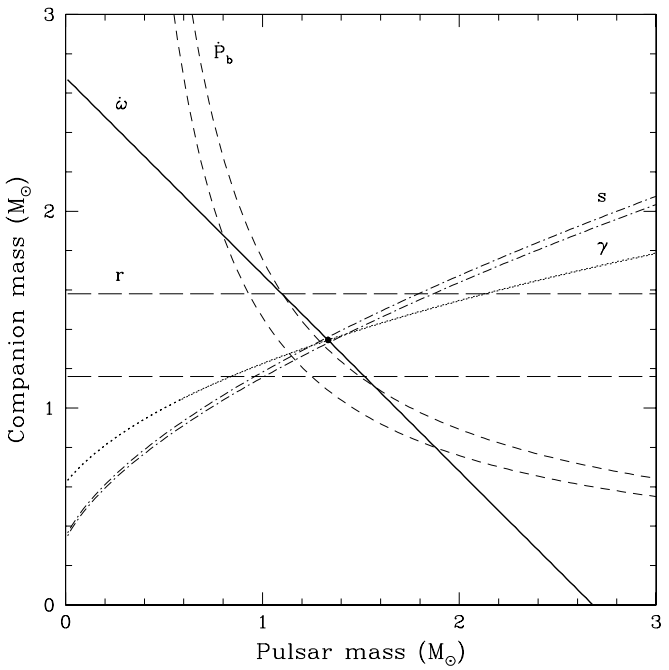

FIG. 6.—Mass-mass diagram for the PSR B1534+12 system. *Labeled curves*: 68% confidence ranges of the DD parameters listed in Table 3. *Filled circle*: Component masses according to the DDGR solution. A kinematic correction for assumed distance $d = 0.7 \pm 0.2$ kpc has been subtracted from the observed value of $\dot{P}_b$; the uncertainty on this kinematic correction dominates the uncertainty of this curve. A slightly larger distance removes the small apparent discrepancy between the observed and predicted values of $\dot{P}_b$.

The Arecibo Observatory, a facility of the National Astronomy and Ionosphere Center, is operated by Cornell University under a cooperative agreement with the National Science Foundation. We thank Zaven Arzoumanian, Fernando Camilo, Andrew Lyne, and David Nice for their earlier contributions to this long-term project, Kiriaki Xilouris, Duncan Lorimer, David Nice, Eric Splaver, Andrea Lommen, Paulo Freire, and Ian Hoffman for assistance with observations, and an anonymous referee for comments on the manuscript. I. H. S. is a Jansky Fellow. S. E. T. is supported by the NSF under grant AST 00-98343. J. H. T. is supported by the NSF under grant AST 96-18357. A. W. is supported by the NSF under grant AST 99-88217.

REFERENCES

Arzoumanian, Z. 1995, Ph.D. thesis, Princeton Univ.
Bell, J. F., & Bailes, M. 1996, ApJ, 456, L33
Camilo F., Thorsett, S. E., & Kulkarni, S. R. 1994, ApJ, 421, L15
Damour T., & Deruelle, N. 1986, Ann. Inst. H. Poincaré, 44, 263
Damour, T., & Taylor, J. H. 1991, ApJ, 366, 501
———. 1992, Phys. Rev. D, 45, 1840
Hankins, T. H., & Rickett, B. J. 1975, in Methods in Computational Physics, Vol. 14 (New York: Radio Astronomy Academic Press), 55
Hulse, R. A., & Taylor, J. H. 1975, ApJ, 195, L51
Kalogera, V., Narayan, R., Spergel, D. N., & Taylor, J. H. 2001, ApJ, 556, 340
Kuijken, K., & Gilmore, G. 1989, MNRAS, 239, 571

Phillips, J. A., & Wolszczan, A. 1991, ApJ, 382, L27
Stairs, I. H., Arzoumanian, Z., Camilo, F., Lyne, A. G., Nice, D. J., Taylor, J. H., Thorsett, S. E., & Wolszczan, A. 1998, ApJ, 505, 352 (Paper I)
Stairs, I. H., Splaver, E. M., Thorsett, S. E., Nice, D. J., & Taylor, J. H. 2000a, MNRAS, 314, 459
Stairs, I. H., Thorsett, S. E., Taylor, J. H., & Arzoumanian, Z. 2000b, in IAU Colloq. 177, Pulsar Astronomy: 2000 and Beyond, ed. M. Kramer, N. Wex, & R. Wielebinski (San Francisco: ASP), 121
Standish, E. M. 1990, A&A, 233, 252
Stinebring, D. R., Kaspi, V. M., Nice, D. J., Ryba, M. F., Taylor, J. H., Thorsett, S. E., & Hankins, T. H. 1992, Rev. Sci. Instrum., 63, 3551
Taylor, J. H. 1987, in General Relativity and Gravitation, ed. M. A. H. MacCallum (Cambridge: Cambridge Univ. Press), 209
———. 1992, Phil. Trans. R. Soc. London, A, 341, 117
———. 1994, Rev. Mod. Phys., 66, 711
Taylor, J. H., & Cordes, J. M. 1993, ApJ, 411, 674
Taylor, J. H., & Weisberg, J. M. 1989, ApJ, 345, 434
Taylor, J. H., Wolszczan, A., Damour, T., & Weisberg, J. M. 1992, Nature, 355, 132
van Kerkwijk, M., & Kulkarni, S. R. 1999, ApJ, 516, L25
Wolszczan, A. 1991, Nature, 350, 688